First-principles studies of cation-doped spinel $LiMn_2O_4$ for lithium ion batteries

Siqi Shi,[1] Ding-sheng Wang,[2] Sheng Meng,[2] Liquan Chen,[1] and Xuejie Huang[1,*]
[1]*Nanoscale Physics and Devices Laboratory, Institute of Physics, Chinese Academy of Sciences, P.O. Box 603, Beijing 100080, China*
[2]*Laboratory for Surface Physics, Institute of Physics, Chinese Academy of Sciences, P.O. Box 603, Beijing 100080, China*
(Received 30 August 2002; published 31 March 2003)

The electronic structure of Cr-doped $LiMn_2O_4$ spinels was investigated from first principles. It was found that the structure of material is more favorable in total energy when the doping chromium atoms are dispersed in $LiMn_2O_4$. With increasing Cr dopant, more electrons are transferred to the oxygen while the positive valence states of Mn atoms are less affected. Consequently, the doping Cr ions possess a higher valence than Mn in $LiMn_2O_4$, agreeing qualitatively with previous experimental results. By combining first-principles methods with basic thermodynamics, average intercalation voltages of this doped system have been calculated. It was found that both the value of the calculated intercalation voltages and their varying trend with increasing Cr dopant are consistent with the experimental facts.

DOI: 10.1103/PhysRevB.67.115130 PACS number(s): 82.47.−a, 61.50.Ah, 61.43.Bn, 71.15.Dx

I. INTRODUCTION

The important characteristics of lithium metal oxides for battery application include the voltage at which lithium is extracted, the amount of lithium that can be reversibly intercalated, and the stability of the material during cycling. Owing to recent developments of high-voltage electrolytes,[1] a high voltage is desirable for obtaining high-energy density. Based on the above advances, seeking the materials with a high intercalation voltage has attracted wide attention. Various substitutions on the transition-metal site have been tried in many structures, including the spinel $LiMn_2O_4$, in order to improve their electrochemical properties, which is promising as an inexpensive and nontoxic positive electrode material for use in lithium-ion batteries. Sigala *et al.*[2] found that the average intercalation voltage increases from 4.05 V to 4.5 V when the chromium content increases in $LiCr_yMn_{2-y}O_4$ from $y=0$ to 1, and concluded that materials with $0<y\leqslant 0.5$ are good candidates for the high-energy and high-voltage positive electrode material. On the other hand, Wu *et al.*[3] found that the valence of Cr ions changes with the Cr-doping content in the $LiMn_2O_4$ spinel by x-ray photoemission spectroscopy (XPS) study. However, to our knowledge, the mechanism of the intercalation voltage's increase and the valence's variation, or the possible relation between the two phenomena, has not yet been reported.

Computational experiments have the advantage for supplementing the real experiments for which one has full control over the relevant variables. What is especially worth mentioning is that first-principles calculations have made an impact on the understanding of practical lithium-ion battery materials. For example, Ceder *et al.*[4] demonstrated that new materials can be prescreened before attempting their synthesis through the first-principles prediction of intercalation voltages. Wolverton and Zunger[5] performed the first-principles prediction of vacancy order-disorder and intercalation battery voltages in Li_xCoO_2. In the present paper we focus on the electronic structure analysis of the chromium-doped $LiMn_2O_4$, in order to elucidate the relation between the electron transfer, the valence change, and the change of the average intercalation voltage of chromium-doped $LiMn_2O_4$.

II. COMPUTATIONAL DETAILS

The electronic structure is calculated in the framework of density-functional theory combined with the local-density approximation (LDA).[6,7] The pseudopotential plane-wave method[8] implemented in the Vienna *ab inito* simulation package (VASP) was used to compute the total energies, the density of states, and the charge density of the undoped and doped $LiMn_2O_4$ spinels. VASP performs an iterative diagonalization of the Kohn-Sham equation of local-density-functional theory based on residuum minimization and optimized charge-density mixing schemes.[9] In our calculations, we used the exchange-correlation functional based on the quantum Monte Carlo simulations of Ceperley and Alder as parametrized by Perdew and Zunger.[10] An optimized ultrasoft Vanderbilt pseudopotential for every atom[11,12] was used in the calculations.

All the calculations were performed in an 8-f.u. $LiMn_2O_4$ supercell with 1−8 Mn atoms replaced by Cr atoms. Owing to the restriction of the computational resources, the experimental geometry of $LiMn_2O_4$ was adopted, neglecting small relaxation during cation doping. The convergence tests of the total energy with respect to the plane-wave energy cutoff and *k*-point sampling have been carefully examined, as shown in Fig. 1. The final set of energies was computed with an energy cutoff of 600 eV and integration using ten *k*-point sampling over the supercell irreducible Brillouin zone, generated by the Monkhorst-Pack scheme.[13]

The theoretical procedure to calculate the average intercalation voltage through first-principles has already been established.[14,15,19] The intercalation voltage is given by

$$V_{\mathrm{AVE}}=-\Delta G/F, \tag{1}$$

where ΔG is the change in Gibbs free energy for the intercalation reaction, and F is the Faraday constant. Assuming that the changes in volume and entropy associated with the intercalation are negligibly small, ΔG can be approximated by the internal energy term ΔE, i.e.,

$$V_{\mathrm{AVE}}\approx -\Delta E/F, \tag{2}$$

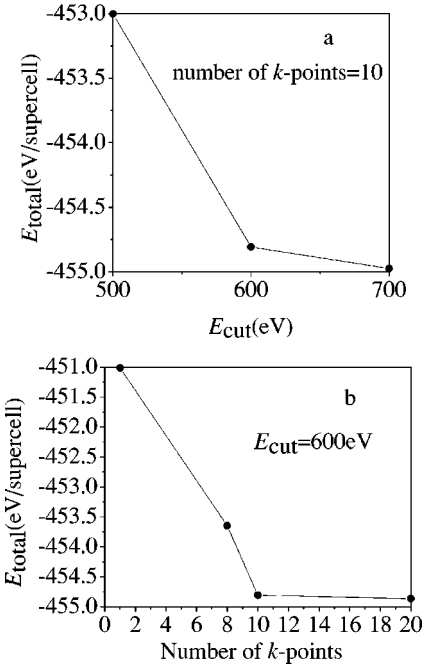

FIG. 1. Total energy E_{total} of 8-f.u. cell $LiMn_2O_4$ supercell as a function of (a) the energy cutoff E_{total} when the number of k points equals 10, and (b) the number of k points in the irreducible zone when E_{cut} equals 600 eV.

where ΔE is given by the difference in total energies between $LiCr_yMn_{2-y}O_4$ and the sum of oxide $Cr_yMn_{2-y}O_4$ and metallic lithium, i.e.,

$$\Delta E = E_{\text{total}}[LiCr_yMn_{2-y}O_4] - E_{\text{total}}[Cr_yMn_{2-y}O_4] - E_{\text{total}}[\text{Li}], \tag{3}$$

where $E_{\text{total}}[LiCr_yMn_{2-y}O_4]$ and $E_{\text{total}}[Cr_yMn_{2-y}O_4]$ are the total energy per formula unit of $LiCr_yMn_{2-y}O_4$ and $Cr_yMn_{2-y}O_4$, respectively. Similarly, the 8-f.u. $Cr_yMn_{2-y}O_4$ supercell is obtained by removing the intercalating Li atoms from the corresponding $8LiCr_yMn_{2-y}O_4$ supercell, also neglecting the relaxation. $E_{\text{total}}[\text{Li}]$ is the total energy of metallic lithium.

III. RESULTS AND DISCUSSION

A. Most probable doping model

In the previous study for the layer intercalation compound $LiCoO_2$[4], because the supercell consists of only a 3-f.u. $LiCoO_2$, all doping configurations for either one or two aluminum atoms in the supercell are equivalent. However, for the present 8-f.u. $LiMn_2O_4$ supercell, 16 manganese positions resulted in multiple nonequivalent cation-doping configurations when more than one Mn atom is replaced by chromium. To avoid the computational complexity in the calculation of ΔE due to enormous doping configurations, choosing a reasonable doping model should be considered theoretically to be a proper approximation. When two Cr atoms are doped into the supercell, there are five nonequivalent doping configurations considering the supercell periodically. Figure 2 shows the total energy of all five nonequivalent doping configurations in this case. The following horizontal coordinate is defined as the minimum distance between the doping Cr atoms taking the supercell periodicity into account:

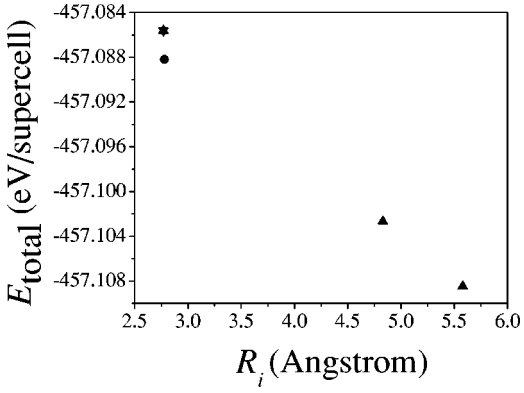

FIG. 2. Total energy E_{total} of 8-f.u. cell $LiMn_2O_4$ supercell as a function of the minimum distance between the two doping chromium atoms. The signs ▲, ▼, and ● represent that the respective configurations are nonequivalent, although R_i is equal.

$$R_i = \min_{j+T \neq i} r_{i,j+T}, \tag{4}$$

where i,j are the indices of Cr atoms in one supercell, and T represents the supercell translation operation. If there are two Cr atoms in each supercell, $R_1 \equiv R_2$, which measures how the doping Cr atoms disperse. We find in Fig. 2 that the configuration, in which the two doping chromium atoms are as far away from each other as possible, is more favorable in energy. Namely, the doping chromium atoms prefer to be dispersed.

Hereby, for the case of doping more than two chromium atoms, we only select the doping configuration in which the sum of the distance R_i over all doping atoms should be maximized. We take this as the most probable doping model and the total energy of this doping configuration is calculated and used in the estimation of the intercalation voltage according to Eqs. (2) and (3).

B. Electronic structure of $LiCr_yMn_{2-y}O_4$

To investigate the role that doping chromium plays in the electronic structure, we calculate the local density of states (DOS) of Mn, Cr, and O in $LiCr_yMn_{2-y}O_4$. In $LiCrMnO_4$, from the point of symmetry all Mn atoms and doping Cr atoms are equivalent, but there are two types of O atoms, one with one Mn and two Cr neighbors, the other with one Cr and two Mn neighbors (see Fig. 10 below). For convenience, two types of O atoms are labeled as O(I) and O(III), respectively. Figures 3 and 4 show the local DOS plots of Mn and O in $LiMn_2O_4$ and $LiCrMnO_4$, respectively. Apparently, the shape of both Mn and O DOS curves remains the same after Cr doping. This is understandable because doping Cr atoms have a similar orbital character to that of the replaced Mn atoms. However, the DOS plots, shown in Figs. 3 and 4, reveal that the Fermi level shifts up with respect to the

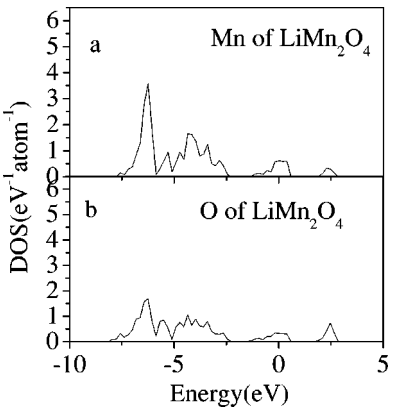

FIG. 3. Local DOS of (a) one Mn atom, and (b) one O atom in $LiMn_2O_4$.

valence-band bottom to about 0.55 eV in $LiCrMnO_4$, compared with the case of $LiMn_2O_4$. This indicates that the number of electrons, which are around O and/or Mn atoms, might increase with increasing Cr content. Actually, this trend in which the Fermi level has been gradually lifted up is found systematically when y increases from 0 to 1.

To reflect the electron transfer quantitatively, we perform the integration of the local DOS from the valence-band bottom to the Fermi level. The integral results are summarized in Table I. The number of electrons around the Mn atoms changes slightly ($<0.01e$) for the highest Cr doping, because there is no direct coupling between $3d$ bands of Mn and the doping chromium. However, we can see 0.077 extra electrons around the O(I) atoms which have two nearest neighbors of doping Cr in $LiCrMnO_4$, and 0.026 extra electrons around the O(III) atoms having only one nearest Cr neighbor, compared with the case of $LiMn_2O_4$. Therefore, most of the extra electrons, which come from Cr atoms, are transferred to oxygen atoms with increasing Cr content. It can be deemed that every O-Cr bond contributes a dipole bearing charge of 0.026 or $0.038e$ (i.e., 0.077/2). Approximately, the charge is considered to be $0.03e$ in the following

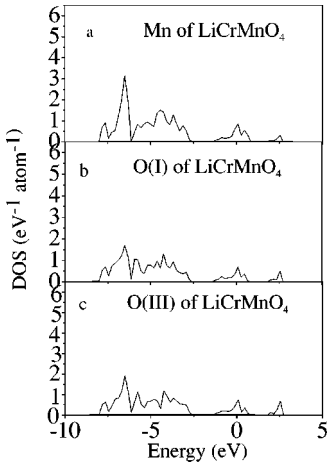

FIG. 4. Local DOS of (a) one Mn atom, (b) one O(I) atom which has one Mn and two Cr neighbors, and (c) one O(III) atom which has one Cr and two Mn neighbors in $LiCrMnO_4$.

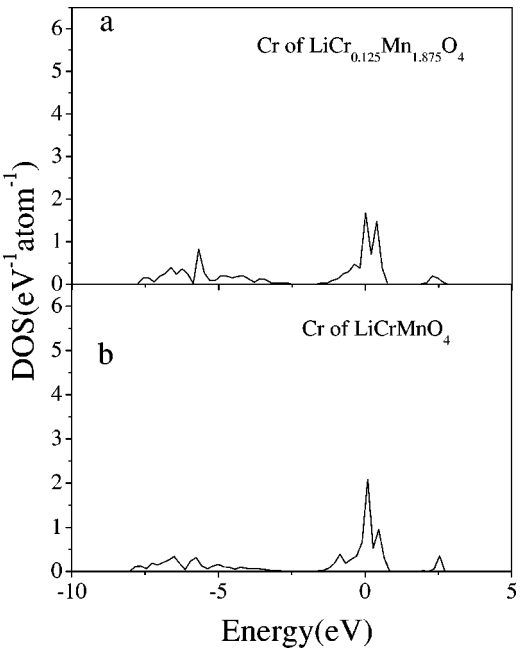

FIG. 5. (a) Local DOS of one Cr atom in $LiCr_{0.125}Mn_{1.875}O_4$; (b) local DOS of one Cr atom in $LiCrMnO_4$.

calculation [see Eq. (5) below]. At the same time, by integrating the local DOS of Cr in $LiCr_{0.125}Mn_{1.875}O_4$ and $LiCrMnO_4$, as shown in Figs. 5(a) and 5(b), we find that the number of the electrons around the Cr atoms decreases by $0.166e$.

Regarding the valence change upon Cr doping, Wu *et al.*[3] observed a core electron level shift using XPS, and found that the core electron level of an Mn ion shifts only slightly. This is consistent with the small change of Mn valency given in the above calculation. Meanwhile, with increasing Cr content, a conversion of Cr^{3+} to Cr^{6+} was also suggested. Although the present theoretical calculation shows the valence increase in qualitative agreement with the experiments, the theoretical valence of Cr increases only by 0.166 when y increases from 0.125 to 1, with a large quantitative difference

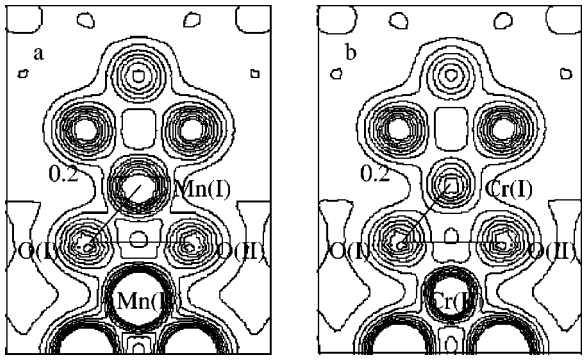

FIG. 6. Charge density (a) on a plane through one Mn(I), nearest-neighboring atoms O(I) and O(II) for $LiMn_2O_4$; (b) on a plane through one Cr(I), nearest neighboring atoms O(I) and O(II) for $LiCrMnO_4$. The number on one contour line shows the electron density in units of $1/Å^3$, and the lines are separated by the linear increment $0.10/Å^3$.

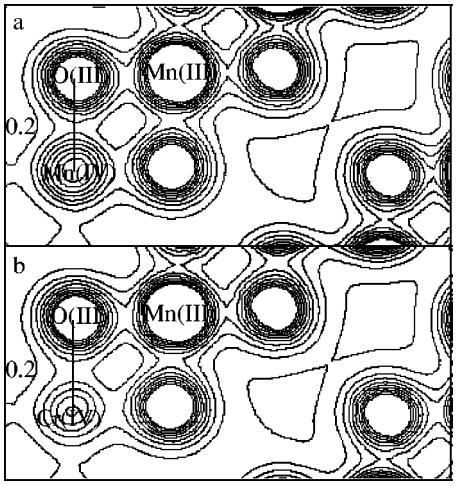

FIG. 7. Charge density (a) on a plane through one O(III), nearest neighboring atoms Mn(III), and Mn(IV) for $LiMn_2O_4$; (b) on a plane through one O(III), near neighboring atoms Mn(III), and Cr(IV) for $LiCrMnO_4$. The number on one contour line shows the electron density in units of $1/Å^3$, and the lines are separated by the linear increment $0.10/Å^3$.

from the experimental results. However, the core electron level shift of O is not experimentally measured, and thus it is hard to judge the experimental overall shift of the potential on the O ions, which could lead to a shift of the Fermi level in the system, which depends mostly on O-2*p* with increasing Cr doping. Therefore, measuring the core electron level of O might help to give a more accurate estimation of Cr ions.

Figure 6(a) shows the charge density on a plane through one Mn(I), near the oxygen atoms O(I) and O(II) for $LiMn_2O_4$. Although Mn(II) is not on the plane, it is also the nearest neighbor to O(I) and O(II). For $LiCrMnO_4$, Mn(I) and Mn(II) are replaced by Cr(I) and Cr(II), respectively, as shown in Fig. 6(b). Similarly, Figs. 7(a) and 7(b) present the charge density on the plane through one O(III), and nearest-neighboring atoms of Mn(III), Mn(IV) for $LiMn_2O_4$, and Cr(IV) for $LiCrMnO_4$. To study the effect of doping chromium atoms on the charge density, we plot the difference in the charge densities for $LiMn_2O_4$ and $LiCrMnO_4$. Because we calculate both $LiMn_2O_4$ and $LiCrMnO_4$ exactly with the same lattice parameters, the charge densities can be subtracted point by point in real space. In Fig. 8, we show the difference in charge density in the range over about the radius of oxygen ions along the lines linking O(I) to Mn(I)/Cr(I), and O(I) to O(II). As can be observed from the plots, there is more charge around oxygen ions for $LiCrMnO_4$.

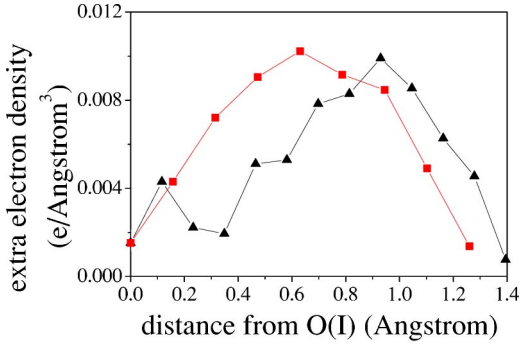

FIG. 8. (Color online) Extra electron density, $\rho[LiCrMnO_4] - \rho[LiMn_2O_4]$, as a function of the distance from O(I), and (▲) along line O(I)-Mn(I)/Cr(I) and (■) along line O(I)-O(II).

Because the extra charge density around the oxygen ion in $LiCrMnO_4$ is well localized, we can determine the extra total electron transfer to the oxygen ion by integrating the extra electron density in an appropriate sphere around the ion, 1.4 Å in radius. We find that about an extra $0.07e$/atom is transferred to the oxygen ion, in agreement with that obtained by partial DOS integration given above. However, from the radius distribution, we believe that these extra electrons go to the O-2*p* orbits.

A previous investigation performed by Mishra and Ceder[16] has shown that the spin-polarization generalized gradient approximation (GGA) is critical for reproducing the orthorhombic $LiMnO_2$ structure as the ground state. For an additional check of our non-spin-polarization LDA results, a spin-polarization GGA calculation using data from Perdew and Wang[17] (PW91) is also carried out on $LiMn_2O_4$ and $LiCrMnO_4$ with the lattice relaxed for energy minimum. Because antiferromagnetism has been observed experimentally,[18] the antiferromagnetic geometry is adopted. For comparison, the results are listed in Table I for the charge transfer. It is clearly seen that the spin polarization and lattice relaxation only give rise to secondary effects regarding charge transfer. The number of electrons and additional dipole moment of Cr-O bonding stay almost the same as the one derived by simple LDA. In fact, non-spin-polarization LDA has been used in the calculations of the cubic spinel.[14,16,19,20]

C. Average intercalation voltage

We calculate the theoretical average intercalation voltages in light of Eqs. (2) and (3) and total energy, as listed in Table II. The comparison of calculated and experimental values is presented in Fig. 9. It is interesting to see that both the the-

TABLE I. Integral number of electrons per atom of the local DOS from the valence-band bottom to the Fermi level. Integral values under spin-polarization GGA are shown in brackets.

System	Mn	O(I)	O(III)	Cr
$LiMn_2O_4$	7.370 (7.365)	6.525 (6.532)	6.525 (6.532)	
$LiCr_{0.125}Mn_{1.875}O_4$				1.516
$LiCrMnO_4$	7.376 (7.369)	6.602 (6.614)	6.551 (6.567)	1.350 (1.338)

TABLE II. Calculated total energies for Li, $LiCr_yMn_{2-y}O_4$, and $Cr_yMn_{2-y}O_4$. ΔE is defined according to Eq. (3). Total energies under spin-polarization GGA are shown in brackets.

System	Total energy (eV/f.u.)	ΔE (eV/f.u.)
Li	-2.044 (-1.920)	
Mn_2O_4	-50.967 (-46.799)	
$LiMn_2O_4$	-56.851 (-52.344)	-3.840 (-3.625)
$Cr_{0.125}Mn_{1.875}O_4$	-51.091	
$LiCr_{0.125}Mn_{1.875}O_4$	-56.995	-3.860
$Cr_{0.25}Mn_{1.75}O_4$	-51.115	
$LiCr_{0.25}Mn_{1.75}O_4$	-57.139	-3.980
$Cr_{0.5}Mn_{1.5}O_4$	-51.232	
$LiCr_{0.5}Mn_{1.5}O_4$	-57.426	-4.150
$Cr_{0.625}Mn_{1.375}O_4$	-51.279	
$LiCr_{0.625}Mn_{1.375}O_4$	-57.563	-4.240
$Cr_{0.75}Mn_{1.25}O_4$	-51.327	
$LiCr_{0.75}Mn_{1.25}O_4$	-57.701	-4.330
$CrMnO_4$	-51.515 (-47.179)	
$LiCrMnO_4$	-57.976 (-53.298)	-4.417 (-4.199)

oretical and experimental average intercalation voltages show an increasing trend as y increases within the range from 0 to 1. In addition, the calculated average intercalation voltages are in agreement with the experimental values available for $LiCr_yMn_{2-y}O_4$. The computation underestimates the intercalation voltages only slightly. Although the reason for this discrepancy has not been clearly determined yet, if the full relaxation is considered, presumably, an even better agreement might be realized. Usually, the underestimate by less than 1 V seems to be a quite universal phenomenon for many oxides when computed using Eq. (2).[19]

In fact, the change of the intercalation voltage upon Cr doping could be estimated by following point-charge interaction approximately as well. A lithium atom couples with six nearest-neighboring O-Cr bonds in LiCrMnO4 (see Fig. 10). The bond angle between each O-Cr and corresponding O-Li bond is 121.19°, and the lengths of the O-Cr and O-Li bonds are 1.96 Å (3.71 a.u.) and 1.95 Å (3.69 a.u.), respectively. Therefore, the distance between Li and Cr is 3.41 Å (6.45 a.u.). Moreover, according to the above electronic structure calculation, the number of extra electron transfers is about 0.03e on each O-Cr bond. Therefore, according to the simple point-charge model (assuming Li ionicity of +1), the total energy difference ΔE_s between $LiCrMnO_4$ and $LiMn_2O_4$ is written as follows:

$$\Delta E_s = 6\times 0.03\times\left[\frac{1}{3.69}-\frac{1}{6.45}\right]\text{hartree}$$

$$= 0.0209 \text{ hartree}$$

$$= 0.57 \text{ eV}. \quad (5)$$

Namely, the intercalation voltage of $LiCrMnO_4$, which is estimated in terms of the simple point-charge model using first-principles data of the O and Cr extra valence, increases by 0.57 V, compared to the case of $LiMn_2O_4$. This is in

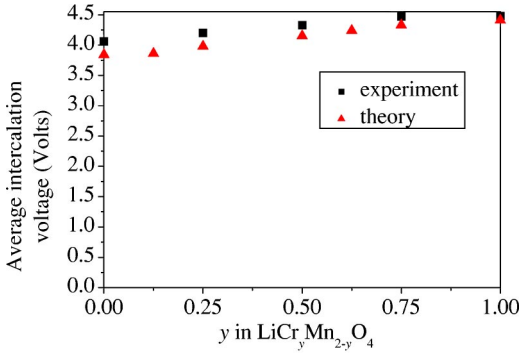

FIG. 9. (Color online) Average intercalation voltage as a function of chromium content. Experimental data are taken from Ref. 2.

remarkable agreement with 0.58 V given by first-principles total-energy calculations and also in good agreement with the 0.42 V provided by our experiments. Hence, it can be concluded that increasing average intercalation voltage with Cr doping is caused by the fact that there are about 0.03 more charges transferred between Cr and O atoms than those between Mn and O atoms, and the energy change is due mostly to the Coulombic interaction between ions.

Our calculations were mostly performed on structure models with atoms occupying the postulated ideal position, since a statistically meaningful coverage of the disorder doping configurations is obviously untraceable from first principles. However, with our present capabilities, one additional check can be added for $LiMn_2O_4$ and $LiCrMnO_4$ systems, which allows the lattice relaxation and using the spin-polarization GGA used by PW91 for the exchange-correlation energy. As shown in Table II, the intercalation voltage is essentially not altered, comparing the non-spin-polarization LDA and model structures with the ideal lattice positions. On the other hand, for non-spin-polarization and antiferromagnetic GGA, the intercalation voltages of $LiMn_2O_4$ calculated in the present work agree well with the values of Mishra and Ceder.[16] The reason even the simple

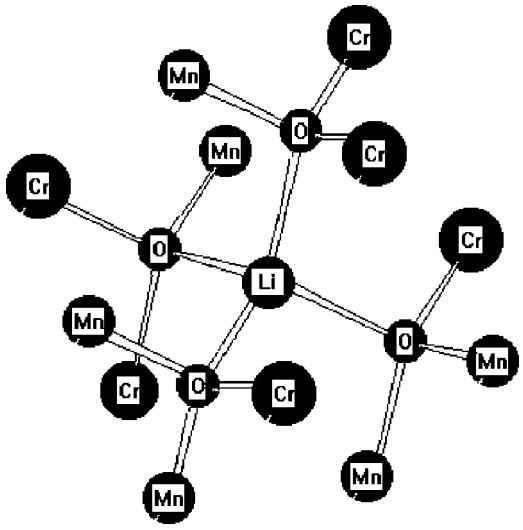

FIG. 10. Cluster configuration around an intercalation Li ion used in the simple point-charge model for $LiCrMnO_4$.

ideal models give rather good results also lies in the Coulombic origin of this intercalation voltage. The Coulombic interaction of the nonmagnetic Li cation and dipole moment of O-Cr(Mn) bonding not only doesn't obviously depend on the spin states of $3d$ Mn(Cr) ions, but also is less sensitive to the small structure relaxation.

IV. SUMMARY

We calculated the electronic structure and average intercalation voltages of $LiCr_yMn_{2-y}O_4$ from first principles. Upon Cr doping, there are about 0.03 extra electrons transferred as well as a stronger dipole moment between Cr and O atoms, compared with that of Mn and O atoms. With increasing chromium content in $LiMn_2O_4$, more Cr-O bondings are formed. Consequently, there is stronger coupling between the lithium ion and Cr-O bonding, thus the intercalation voltage increases. The average voltages calculated from first-principles methods are in good agreement with our experimental values. Finally, the simple point-charge model is used to estimate the change of the intercalation voltage upon Cr doping, and also gives the same varying trend as that of the experimental facts. This shows that the energy change, and the subsequent intercalation voltage change, is of Coulombic origin, and also the first-principles calculation reveals charge transfer between the doping ion and the host, which is essential to the study of this material.

ACKNOWLEDGMENTS

This work is supported by the National Science Foundation of China (NSFC) (Grant No. 59972041) and the National 863 key program (Grant No. 2001AA32301). Dingsheng Wang is supported by Pan-deng Project No. G19990328-2. The author wishes to express his sincere thanks to Dr. L. F. Xv.

*Electronic address: xjhuang@aphy.iphy.ac.cn

[1] J. M. Tarascon and D. Guyomard, Solid State Ionics **69**, 293 (1994).
[2] C. Sigala, D. Guyomard, A. Verbaere, Y. Piffard, and M. Tournoux, Solid State Ionics **81**, 167 (1995).
[3] Chuan Wu, Zhaoxiang Wang, Feng Wu, Liquan Chen, and Xuejie Huang, Solid State Ionics **69**, 293 (2001).
[4] G. Ceder, Y. -M. Chiang, D. R. Sadoway, M. K. Aydinol, Y. -l. Jang, and B. Huang, Nature (London) **392**, 694 (1998).
[5] C. Wolverton and A. Zunger, Phys. Rev. Lett. **81**, 606 (1998).
[6] P. Hohenberg and W. Kohn, Phys. Rev. B **136**, B864 (1964).
[7] W. Kohn and L. J. Sham, Phys. Rev. A **140**, A1133 (1965).
[8] G. Kresse and J. Hafner, Phys. Rev. B **48**, 13 115 (1993); *ibid.* **49**, 14 251 (1994).
[9] G. Kresse and J. Furthmuller, Phys. Rev. B **54**, 11 169 (1996).
[10] J. P. Perdew and A. Zunger, Phys. Rev. B **23**, 5048 (1981).
[11] D. Vanderbilt, Phys. Rev. B **41**, 7892 (1990).
[12] G. Kresse and J. Hafner, J. Phys.: Condens. Matter **6**, 8245 (1994).
[13] H. J. Monkhorst and J. D. Pack, Phys. Rev. B **13**, 5188 (1976).
[14] G. Ceder, M. K. Aydinol, and A. F. Kohn, Comput. Mater. Sci. **8**, 161 (1997).
[15] C. Wolverton and A. Zunger, Phys. Rev. B **57**, 2242 (1998).
[16] S. K. Mishra and G. Ceder, Phys. Rev. B **59**, 6120 (1999).
[17] J. P. Perdew *et al.*, Phys. Rev. B **46**, 6671 (1992).
[18] C. Masquelier, M. Tabuchi, K. Ado, R. Kanno, Y. Kobayashi, Y. Maki, O. Nakamura, and J. B. Goodenough, J. Solid State Chem. **123**, 255 (1996).
[19] M. K. Aydinol, A. F. Kohn, G. Ceder, K. Cho, and J. Joannopoulos, Phys. Rev. B **56**, 1354 (1997).
[20] M. K. Aydinol and G. Ceder, J. Electrochem. Soc. **144**, 3832 (1997).